Atmospheric Aerosol Measurements at the Pierre Auger Observatory

Laura Valore* **for the Pierre Auger Collaboration**

**Universitá degli Studi di Napoli "Federico II" and INFN Napoli*

Abstract**. The Pierre Auger Observatory uses the atmosphere as a huge calorimeter. This calorimeter requires continuous monitoring, especially for the measurements made with the fluorescence telescopes. A monitoring program with several instruments has been developed. LIDARs at the sites of each of the fluorescence detectors are used to measure aerosols and clouds. Beams from calibrated laser sources located near the centre of the Observatory are used to measure the light attenuation due to aerosols, which is highly variable even on time scales of one hour. The Central Laser Facility (CLF) has been used to provide hourly aerosol characterisations over five years based on two independent but fully compatible procedures. The eXtreme Laser Facility (XLF), located in a symmetric position relative to the CLF and the four fluorescence detector sites, has just started operation. The level of cloud coverage is measured using cameras sensitive to the infrared and can also be detected with the sky background data.**

Keywords**: atmospheric monitoring, aerosols, clouds**

I. INTRODUCTION

Primary cosmic rays at ultrahigh energies (E $>$ 10^{18}eV) cannot be observed directly because of their extremely low flux. The properties of primary particles (energy, mass composition, arrival direction) are deduced from the study of the cascade of secondary particles originating from their interaction with air molecules. The Pierre Auger Observatory is a hybrid detector with an array of more than 1600 surface detectors overlooked by 24 fluorescence telescopes grouped in 4 sites each with 6 telescopes at the array periphery. The Fluorescence Detector (FD) is designed to perform a nearly calorimetric measurement of the energy of cosmic ray primaries, since the fluorescence light emitted by nitrogen air molecules excited by shower charged particles is proportional to the energy loss of the particles. Due to the constantly changing properties of the calorimeter (i.e. the atmosphere), in which the light is both produced and through which it is transmitted, a huge system with several instruments has been set up to perform a continuous monitoring of its properties. In particular aerosols are highly variable on a time scale of one hour. We perform measurements of the aerosol parameters of interest: the aerosol extinction coefficient $\alpha(h)$, the vertical aerosol optical depth $\tau_a(h)$, the normalised differential cross section $P(\theta)$ (or phase function), and the wavelength dependence of the aerosol scattering parametrised by the Ångstrom coefficient γ. Recent results showing that cloud coverage has a major influence on the reconstruction of air showers has led to a special effort in clouds monitoring.

II. THE AEROSOL MONITORING SYSTEM

The Pierre Auger Observatory operates an array of monitoring devices to record the atmospheric conditions. Most instruments are used to estimate the hourly aerosol transmission between the point of production of the fluorescence light and the Fluorescence Detectors and for the detection of clouds. If not properly taken into account, these dynamic conditions can bias the showers reconstruction. A map of the Pierre Auger Observatory aerosol monitoring system is shown in fig. 1.

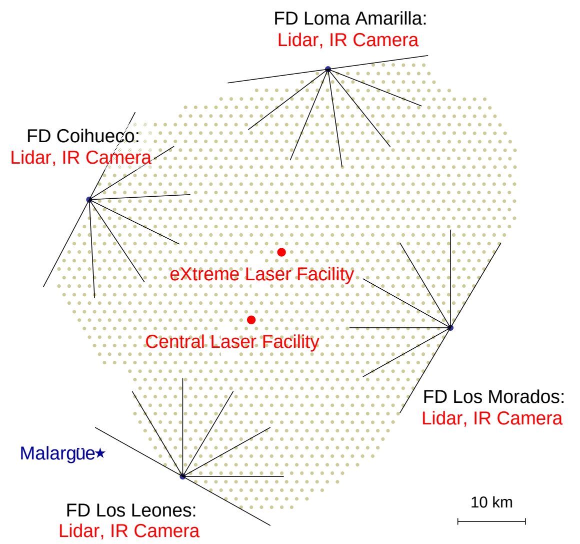

Fig. 1. Atmospheric monitoring devices map

In this paper, systems measuring aerosol optical depth and clouds, which are the main sources of uncertainties, are described. The aerosol optical depth contributes to the uncertainty on energy from 3.6% at E = $10^{17.5}$ eV to 7.9% at E = 10^{20} eV, and to the uncertainty on the depth of the shower maximum (X_{max}) from 3.3 g cm^{-2} at E = $10^{17.5}$ eV to 7.3 g cm^{-2} at E = 10^{20} eV. The phase function and wavelength dependence contribute 1% and 0.5% in energy and 2% and 0.5% in X_{max}, respectively [2]. Clouds can distort the light profiles of showers, and give a significant contribution to the hybrid exposure of the detector and therefore to the hybrid spectrum.

The Central Laser Facility (CLF) [1] produces calibrated UV laser beams every 15 minutes during FD data acquisition from a position nearly equidistant from three out of four FDs. A similar facility, the eXtreme Laser Facility (XLF), was completed in November 2008, at a symmetric position with respect to the CLF and the FDs. Both systems can produce vertical and inclined laser beams at 355 nm, having a nominal energy of 7 mJ per pulse, which is approximately equivalent to the amount of fluorescence light produced by a 10^{20} eV shower. The number of photons reaching the FDs depends on the number of photons at the source and on the atmospheric conditions between the laser and the detector. Using the independently measured laser pulse energy, the aerosol transmission can be inferred. Clouds along the laser beam and between the laser site and the FDs can be identified.

Four elastic backscatter LIDAR stations are operating (the last one since May 2008). Each station has a fully steerable frame equipped with a UV laser, mirrors and PMTs for the detection of the elastic backscattered light. During FD data taking, hourly sets of scans are performed out of the FDs field of view to avoid interference with the FD telescopes to record local aerosol conditions and clouds. Elastic LIDARs also provide a rapid monitoring mode after the detection of events of particular physical interest, scanning very high-energy showers tracks within 10 minutes from detection (Shoot the Shower, StS) [5]. In addition, the Los Leones LIDAR station is equipped with a vertical Raman LIDAR system, detecting the inelastic Raman backscattered light. The molecular Raman cross section is small, therefore during Raman runs the laser is fired at high power to collect enough light. To avoid interference with the FD, Raman LIDAR runs are limited to 20 minutes at the beginning and 20 minutes at the end of the FD acquisition.

A Raytheon 2000B infrared cloud camera (IRCC) with a spectral range from 7 to 14 μm is located on the roof of each FD building to determine the cloud coverage. Each IRCC is housed within a weather protective box and is mounted on a pan-and-tilt device. During FD data acquisition, each IRCC takes a picture of the field of view of the 24 telescopes every 5 minutes, to flag pixels “covered” by clouds. In addition, a full sky scan is performed every 15 minutes to take a photograph of the entire sky above each FD site. A bi-dimensional map of the sky is produced.

Two techniques based on the analysis of FD background data recorded during acquisition have also been developed to retrieve cloud coverage information. Clouds can be identified by studying the changes in the brightness of the night UV sky, appearing as very dark patches against the bright night sky. The FD background data and IRCC analyses are complementary with the LIDAR and CLF studies that provide the height of cloud layers to achieve a better accuracy in cloud studies and obtain a 3-dimensional map of the sky.

III. AEROSOL OPTICAL DEPTH MEASUREMENTS

The light scattered out of the CLF beam produces tracks recorded by the FD telescopes. Laser light is attenuated in its travel towards FDs as the fluorescence light emitted by a shower. Therefore, the analysis of the amount of CLF light that reaches the FD building can be used to infer the attenuation due to aerosols, once the nominal energy is known. An hourly aerosol characterisation is provided in the FD field of view with two independent approaches using the same vertical laser events. The first method (Data Normalised Analysis) consists of an iterative procedure that compares hourly average profiles to reference profiles chosen in extremely clear (aerosol free) nights. The procedure starts with the definition of an average hourly profile obtained merging the corresponding four quarter-hour profiles.

A first estimate of $\tau_a(h)$ is given by:

$$\tau_a^{\rm first}(h) = -\frac{\ln\left(I_{\rm hour}(h)/I_{\rm aerfree}(h)\right)}{1+1/\sin\theta}$$

where $I_{\rm hour}$ is the average hourly laser profile, $I_{\rm aerfree}$ is the reference profile and θ is the elevation angle of the laser track point at height h. This calculation does not take into account the laser beam scattering due to aerosols; to overcome this, $\tau_a^{\rm first}(h)$ is differentiated to calculate the extinction $\alpha(\rm h)$ over short intervals in which the aerosol scattering conditions change slowly. Finally, $\tau_a(h)$ is estimated re-integrating $\alpha(h)$.

The second procedure (Laser Simulation Analysis) compares quarter-hour CLF profiles to simulated laser events generated varying over more than 1100 aerosol conditions to find the best compatibility. Aerosol-free profiles are used to fix the energy scale between simulations and real events. A parametric model of the aerosol attenuation is adopted, described by the Horizontal Attenuation Length ($\rm L_{mie}$) and the Scale Height ($\rm H_{mie}$) :

$$\tau_a(h) = -\frac{H_{mie}}{L_{mie}}\left[e^{\left(-\frac{h}{H_{mie}}\right)} - e^{\left(-\frac{h_0}{H_{mie}}\right)}\right]$$

where $\rm h_0$ is the altitude above sea level of the detector.

Aerosol-free nights are needed as a reference in both analyses. A procedure to identify these extremely clear conditions in real data has been developed: the shape of each real profile is compared to the one of an aerosol-free simulated profile using a Kolmogorov test that checks their compatibility. The profile with the highest probability is chosen as the reference. Aerosol-free conditions occur more frequently during austral winter.

An example of the good agreement between a typical hourly vertical aerosol optical depth profiles measured with the Data Normalised and the Laser Simulation analyses is shown in figure 2.

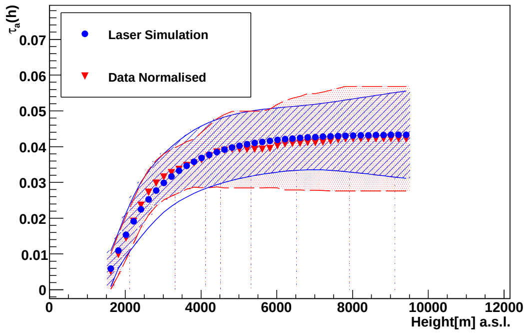

Fig. 2. Comparison of a $\tau_a(h)$ profile estimated by the Laser Simulation and the Data Normalised analyses

The results produced with these two independent analyses are fully compatible, as shown in fig. 3: the average τ_a(3 km) above the detector in the period from January 2005 to December 2008 is 0.04 $\pm$ 0.01.

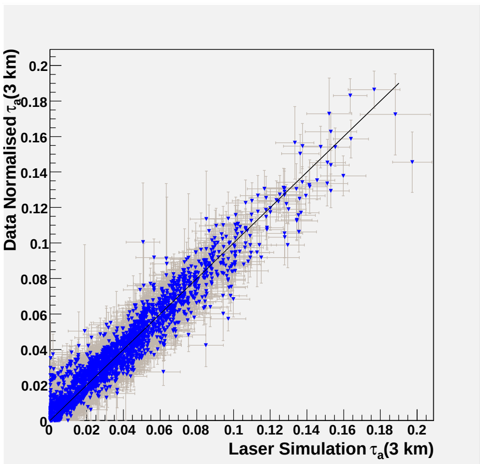

Fig. 3. $\tau_\mathrm{a}(\mathrm{h})$ estimated by CLF analyses

By studying the vertical aerosol optical depth as a function of time, over a period of 4 years of data, a clear seasonal variation is observed, as shown in figure 4. Austral winter is the season with lower aerosol attenuation.

In addition to the CLF estimate of aerosol conditions, the four LIDAR stations provide a local estimate of $\tau_\mathrm{a}(\mathrm{h})$ and $\alpha(\mathrm{h})$ using a multiangular inversion procedure [4]. Every hour, the LIDAR telescopes sweep the sky in a set pattern, pulsing the laser at 333 Hz and observing the backscattered light with the optical receivers. However, except for the StS mode [5] and a short hourly set of horizontal shots towards CLF, the LIDAR laser beams point outside the FD telescopes field of view to avoid triggering the detector.

IV. Clouds Detection

Clouds have a significant impact on shower reconstruction, blocking the transmission of light in its travel from the emission point to the fluorescence telescopes,

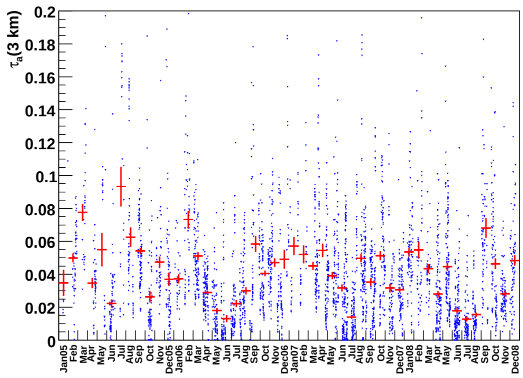

Fig. 4. $\tau_\mathrm{a}(3\mathrm{km})$ as a function of time. Lower values of $\tau_\mathrm{a}(3\mathrm{km})$ happen in austral winter (June - July)

or enhancing the amount of light scattered towards the FD, depending on the position of the cloud itself.

The cloud coverage can be determined by analysing the FD background data: the variance of the baseline fluctuation is recorded every 30 s, providing a reasonable estimate of the changes in the brightness of the sky. As already mentioned, two approaches have been developed. "Star Visibility Method" : as stars are visible in the background data, it is possible to predict at what time a particular star would be visible. A null detection of the star indicates the presence of a cloud in the field of the viewing pixel. "Background Variation Method" : clouds are good absorbers of UV radiation, therefore they appear as dark areas against the bright background of the UV night sky. Sudden drops of the brightness of a part of the sky are an indication of an obscuring cloud. In fig. 5, an example of change in brightness from a single pixel during one night is shown: the peaks are stars crossing the field of view, while the drops are likely to be clouds.

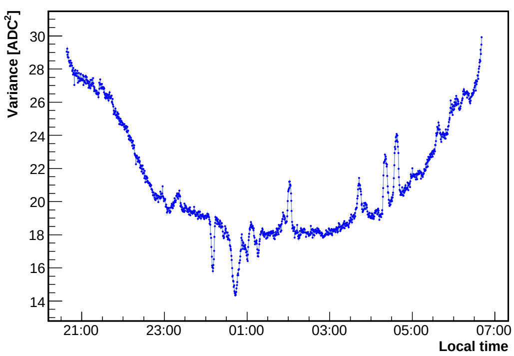

Fig. 5. Typical night sky background variation from one pixel

The four IRCCs record the cloud coverage making a photograph of the field of view of each telescope every 5 minutes during FD acquisition. The image data are processed and a coverage mask is created for each pixel of the telescope to identify cloud covered

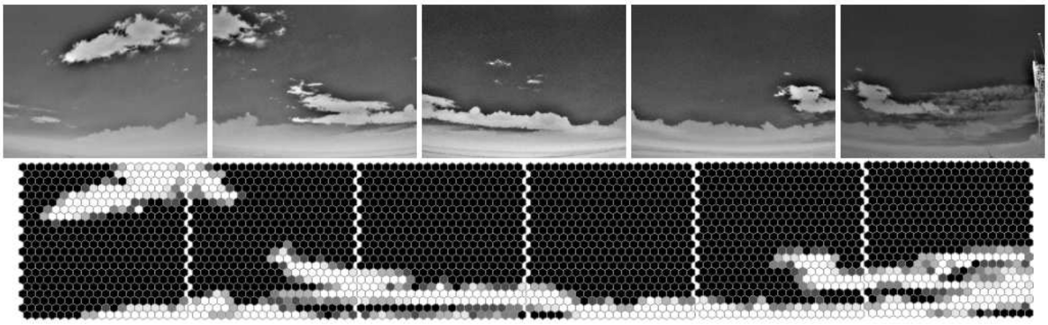

Fig. 6. Top: raw IRCC image. Bottom: FD pixels coverage mask: lighter values on the greyscale represent greater cloud coverage

pixels to be removed from the shower reconstruction procedure. Cloud cameras are not radiometric, therefore each pixel value is proportional to the difference between the temperature in the viewing direction and the average temperature of the entire scene. In fig. 6, the raw IRCC images of the FD field of view are shown together with the final mask. The database is filled with the coverage for each pixel in the map.

While the IR cloud cameras and the FD background data analyses record the cloud coverage in the FD field of view, they cannot determine cloud heights, that must be measured using the LIDAR stations and CLF. In cloud detection mode, LIDAR telescopes sweep the sky with a continuous scan in two orthogonal paths with fixed azimuthal angle, one of which is along the central FD azimuth angle, with a maximum zenith angle of $45°$. The full scan takes 10 minutes per path. Clouds are detected as strong localised scattering sources, and the timing of the scattered light is related to the cloud height. The cloud finding algorithm starts with the subtraction of the expected signal for a simulated purely molecular atmosphere ($S_{\rm mol}$) to the real one ($S_{\rm real}$). The obtained signal is approximately constant before the cloud, and has a non-zero slope inside the cloud. A second-derivative method to identify cloud candidates and obtain cloud thickness is applied. LIDARs provide hourly information on cloud coverage and height.

In fig. 7, the intensity of the backscattered light as a function of height and horizontal distance from the LIDAR station is shown.

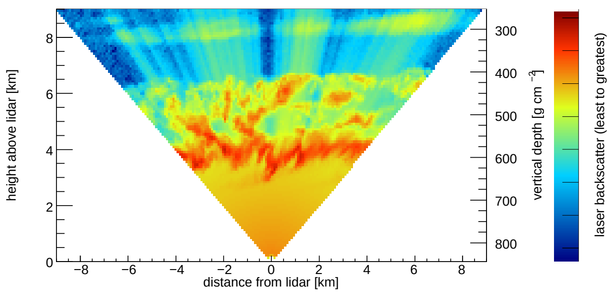

Fig. 7. A cloud layer around 3.5 km height as detected by the LIDAR

The Central Laser Facility and the eXtreme Laser Facility can be used to detect clouds along the vertical laser path and between their position and the FDs, looking at the profiles of photons collected at the FD buildings, since clouds can enhance or block the trasmitted light, depending of their position. A cloud positioned directly along the vertical laser track will scatter a greater amount of light in every direction, producing a peak in the light profile. In this case the cloud is directly above the laser facility site, and timing of the scattered light is related to the cloud height allowing to define the height of the cloud layer. If clouds are between the laser source and the FD, a local decrease in the laser light profile is observed. In this case the timing of the received light is not directly related to the cloud height, and only the cloud coverage in the FD field of view can be defined. A database is filled with the informations on the height of the observed cloud layers.

V. Conclusions

The Pierre Auger Observatory operates a huge system to provide continuous measurements of the highly variable aerosol attenuation and for the detection of clouds, main sources of uncertainties in the shower reconstruction. The highest energy air showers are viewed at low elevation angles by the Fluorescence Detectors and through long distances in the lower part of the atmosphere, where aerosols are in higher concentration and therefore the aerosol attenuation becomes increasingly important. Also clouds have a significant effect on shower reconstruction. All the described instruments are operating, and most of the results are currently used in the reconstruction of shower events.

References

[1] B. Fick et al., *The Central Laser Facility at the Pierre Auger Observatory*, JINST 1:P11003, 2006.

[2] S.Y. BenZvi [Pierre Auger Collaboration], *Atmospheric Monitoring and its use in Air Shower Analysis at the Pierre Auger Observatory*, Proc. 31th ICRC

[3] J. Abraham et al., *A Study of Molecular and Aerosol Conditions at the Pierre Auger Observatory*, submitted to Astropart. Phys. 2009.

[4] S.Y. BenZvi et al., *The Lidar System of the Pierre Auger Observatory*, Nucl. Instrum. Meth., A574:171-184, 2007

[5] B. Keilhauer [Pierre Auger Collaboration], *Rapid Monitoring of the atmosphere after the detection of high-energy showers at the Pierre Auger Observatory*, Proc. 31th ICRC